Supporting Information

69451 Weinheim, Germany

Triple salting-out effect: a required phenomenon in the formation of ionic-liquid-based aqueous multiphase systems

Helena Passos, Sara H. Costa, Ana M. Fernandes, Mara G. Freire, Robin D. Rogers, João A.P. Coutinho*

Abstract: Novel aqueous multiphase systems (MuPS) formed by quaternary mixtures composed of cholinium-based ionic liquids (ILs), polymers, inorganic salts and water are here reported. The influence of several ILs was studied, demonstrating that a triple salting-out is a required phenomenon to prepare MuPS. The respective phase diagrams and “tie-surfaces” were determined, followed by the evaluation of the effect of temperature. Finally, it is shown the remarkable ability of IL-based MuPS to selectively separate a complex mixture of textile dyes.

DOI: 10.1002/anie.2016XXXXX

Table of Contents

Experimental Procedure

Materials. The determination of the liquid-liquid quaternary phase diagrams was performed using tri-potassium phosphate, K_3PO_4 (98 wt % pure) from Sigma, polyethylene glycol with an average molecular weight of 600 g mol^{-1} (PEG 600) from Sigma-Aldrich, polypropylene glycol with an average molecular weight of 400 g·mol^{-1} (PPG 400) from Aldrich, and the following cholinium ([$N_{111(2OH)}$])-based ionic liquids (ILs): cholinium butanoate, [$N_{111(2OH)}$][But], cholinium propanoate, [$N_{111(2OH)}$][Pro], cholinium lactate, [$N_{111(2OH)}$][Lac], cholinium acetate, [$N_{111(2OH)}$][Ace] (98 wt % pure), cholinium glycolate, [$N_{111(2OH)}$][Gly], cholinium dihydrogenphosphate, [$N_{111(2OH)}$][DHP] (99 wt % pure) and cholinium chloride, [$N_{111(2OH)}$]Cl (≥ 98 wt %). The chemical structures of the investigated ILs are presented in Figure S1. [$N_{111(2OH)}$][Ace] was supplied by Iolitec, while [$N_{111(2OH)}$]Cl was provided by Sigma. [$N_{111(2OH)}$][Lac], [$N_{111(2OH)}$][Gly], [$N_{111(2OH)}$][Pro], and [$N_{111(2OH)}$][But] were synthesized in our lab according to well established procedures.[1,2] To reduce the volatile impurities to negligible values and remove traces of water, individual samples of each IL were dried at moderate temperature (≈ 50 °C) and at high vacuum (≈ 10 ^{5} Pa), under constant stirring, and for a minimum period of 24 h. After this procedure, the purity of each IL was further checked by ^{1}H and ^{13}C NMR spectra and found to be > 98 wt %. The textile dyes sudan III and chloranilic acid were acquired from Merck, while Prussian blue pigment (PB) 27 was aquired from Holliday Pigment. The food additive tartrazine (E102) was from Globo. The additional biomolecules studied are gallic acid (99.5 wt % pure) from Merck, caffeine (99 wt % pure) and -tyrosine (99 wt % pure) from Fluka, -tryptophan (99 wt % pure) and - phenylalanine (99 wt % pure) from Sigma-Aldrich, vanillin (99 wt % pure) and glycine (99 % pure) from Acros Organics, and -ascorbic acid (99.7 wt % pure) from Analar. The chemical structures of the extracted dyes are presented in Figure S2. The water used was double distilled, passed through a reverse osmosis system, and further treated with a Milli-Q plus 185 apparatus.

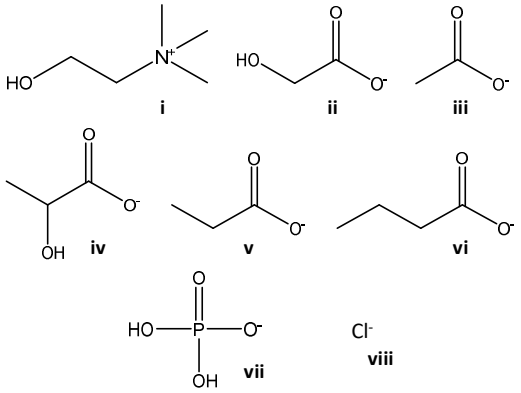

Figure S1. Chemical structures of the cation and anions that constitute the studied ILs: (i) [$N_{111(2OH)}$]$^{+}$; (ii) [Gly]$^{-}$; (iii) [Ace]$^{-}$; (iv) [Lac]$^{-}$; (v) [Prop]$^{-}$; (vi) [But]$^{-}$; (vii) [DHP]$^{-}$; (viii) Cl^{-}.

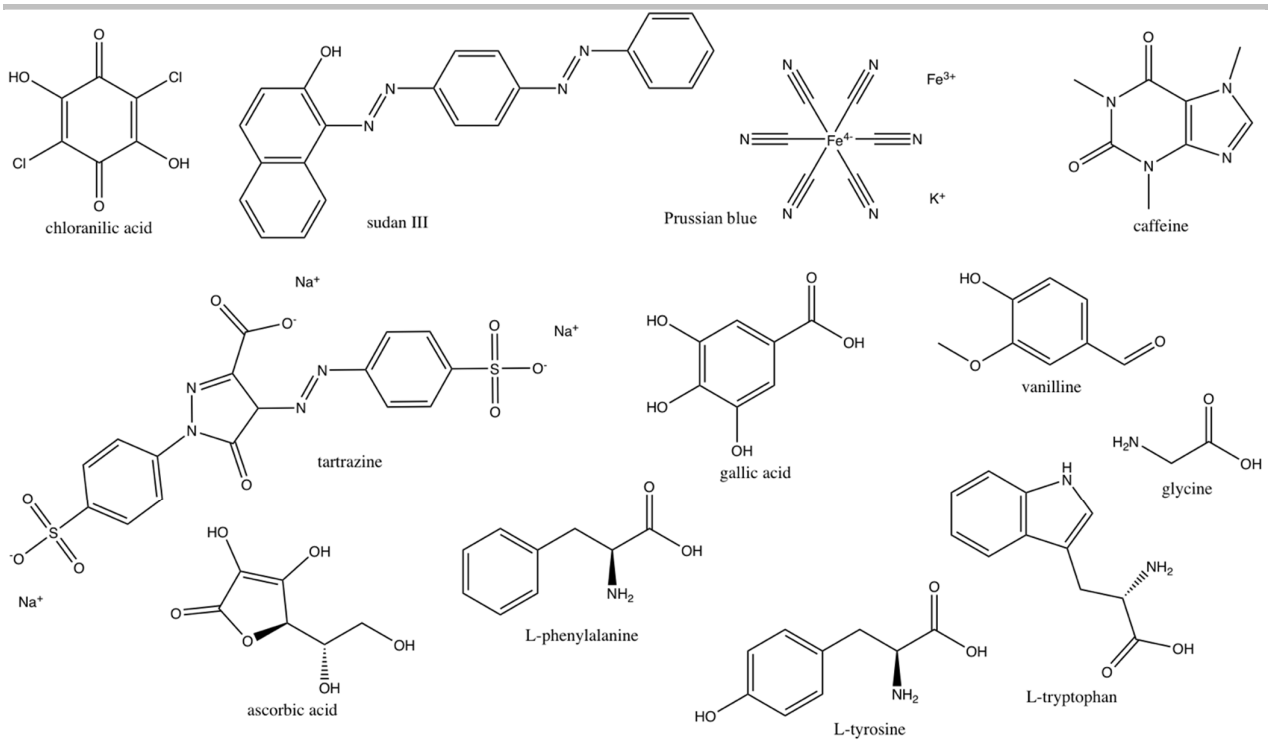

Figure S2. Chemical structures of dyes and other biomolecules separated with MuPS.

Determination of ternary phase diagrams (aqueous biphasic systems). The experimental phase diagrams investigated in this work were determined by the cloud-point titration method[3,4] at (25 ± 1) °C and atmospheric pressure. Aqueous solutions of K_3PO_4 at 50 wt % and aqueous solutions of $[N_{111(2OH)}]Cl$ and PEG at several mole fractions (0.08, 0.31, 0.49, 0.55, 0.82 and 0.95 moles of $[N_{111(2OH)}]Cl$ *per* total moles) were prepared gravimetrically (± 10^{-4} g) and used to determine the binodal curves. Repetitive drop wise addition of the aqueous inorganic salt solution to each aqueous solution of $[N_{111(2OH)}]Cl$/PEG was carried out until the detection of a cloudy solution, followed by the drop wise addition of ultra-pure water until the detection of a single and limpid phase. The whole procedure was performed under constant stirring and the quaternary system compositions were determined by the weight quantification of all the components added. The same procedure was executed to determine the solubility curves of the ternary systems composed of PEG 600 + K_3PO_4 + H_2O and $[N_{111(2OH)}][Lac]$ + K_3PO_4 + H_2O.

For the system composed of $[N_{111(2OH)}][Gly]$ + K_3PO_4 + H_2O and $[N_{111(2OH)}][DHP]$ + K_3PO_4 + H_2O the turbidimetric method was used.[5] Several mixtures of the system at the biphasic region were initially prepared. Under constant stirring, ultra-pure water was added until the detection of a clear and limpid solution (monophasic region). Each mixture corresponds to one point of the binodal curve. The mixture compositions were gravimetrically determined within ±10^{-4} g and at (25 ± 1) °C. The same procedure was used to determine the limit between the three phases region and the biphasic region, and the solid-liquid region and the three phases region. The 3D representations of $[N_{111(2OH)}]Cl$-based MuPS were carried out using the Origin Pro 9.1.0 software, from Origin Lab Corporation.

Determination of the coexisting phases composition. Mixtures at the triphasic region were gravimetrically prepared with $[N_{111(2OH)}]$-based ILs + PEG + K_3PO_4 + H_2O, vigorously stirred, and allowed to equilibrate for at least 12 h at (25 ± 1) °C. After the three-phase separation, each phase was weighted and further analytically quantified. The water content in each phase was determined by a gravimetric approach, *i.e.* by the evaporation of water until constant weight in an air oven at ± 105 °C. The $[N_{111(2OH)}]^+$ cation quantification was carried out using a Micromass Quattro LC triple quadrupole mass spectrometer using a calibration curve previously established. The operating conditions of the mass spectrometer were the following: source and desolvation temperatures of 80 °C and 150 °C, respectively; capillary voltage of 3000 V; and cone voltage of 30 V. N_2 was used as the nebulization gas and the diluted samples (50:1000, v/v) were introduced at a 10 mL min^{-1} flow rate using the methanol–water (1:1, v/v) mixture as the eluent solvent. For the measurement of peak abundances, an average of 100 scans for each mass spectrum was used. Triplicate independent sampling measurements were performed for both standards and samples. The chloride anion content was determined using a chloride ion selective electrode. The potassium and phosphonium contents were determined by inductively coupled plasma-optical emission spectrometry (ICPOES) using a Jobin Yvon 70 plus, power 880 W, under a plasma gas flow of 16 mL min^{-1} and pressure of 2.6 bar. For the remaining $[N_{111(2OH)}]$-based MuPS the coexisting phases were identified through the determination of their electrical conductivity at (25 ± 1) °C, using a Mettler Toledo SevenMultiTMdual pH/conductivity meter.

SUPPORTING INFORMATION

Selective extraction of dyes and other biomolecules. Different dyes and biomolecules were studied as model molecules to demonstrate the potential application of MuPS. Quaternary mixtures, with a common composition and within the triphasic region of the phase diagrams investigated, were prepared: 23 wt % of PEG + 23 wt % of [$N_{111(2OH)}$]-based IL + 23 wt % K_3PO_4 + 31 wt % of H_2O (or biomolecule aqueous solution) and 21 wt % of PEG + 20 wt % of [$N_{111(2OH)}$][DHP] + 30 wt % K_3PO_4 + 29 wt % of H_2O (or biomolecule aqueous solution). A small amount of each dye (≈ 0.30 mg of chloranilic acid, sudan III, PB 27 or tartrazine) was added to glass tubes containing the quaternary mixtures with a total weight of 3 g. In the case of biomolecules, aqueous solutions of each biomolecule were prepared at the following concentrations: 3.57 x 10^{-3} mol·L^{-1} for -tryptophan, 1.82 x 10^{-3} mol·L^{-1} for -tyrosine, 3.36 x 10^{-3} mol·L^{-1} for -phenylalanine, 9.93 x 10^{-2} mol·L^{-1} for glycine, 8.14 x 10^{-3} mol·L^{-1} for gallic acid, 3.48 x 10^{-3} mol·L^{-1} for vanillin, 7.70 x 10^{-3} mol·L^{-1} for ascorbic acid, and 4.39 x 10^{-3} mol·L^{-1} for caffeine. All mixtures were centrifuged during 10 min at 2000 rpm to achieve the complete phase separation. After a careful separation of the phases, the quantification of each dye was carried by UV-spectroscopy using a synergy/HT microplate reader at a wavelength of 321 nm for chloranilic acid, 510 nm for sudan III, 600 nm for PB27, 400 nm for tartrazine, 275 nm for -tryptophan, 292 nm for -tyrosine, 257 nm for -phenylalanine, 262 nm for gallic acid, 249 nm for vanillin, 300 nm for ascorbic acid and 272 nm for caffeine. To quantify the glycine present in each phase, 75 µL of ninhydrin reagent was added to 100 µL of an adequately diluted sample of each phase. After incubation at 80 °C during 30 min, ethanol at 50 % (v/v) was added to stop the reaction. Then glycine was quantified by UV-spectroscopy at a wavelength of 570 nm.[6,7] Calibration curves for all dyes and biomolecules were previously established and blank controls always used. The extraction efficiencies of each molecule to a specific phase is defined as the ratio between the amount of dye or biomolecule in that phase and that in the total mixture.

SUPPORTING INFORMATION

Results and Discussion

Aqueous biphasic systems phase diagrams

Table S1. Experimental binodal data for systems composed of [$N_{111(2OH)}$]-based ILs (1) + K_3PO_4 (2) + H_2O (3) at 25 °C and atmospheric pressure.

[$N_{111(2OH)}$][Lac]		**[$N_{111(2OH)}$][Gly]**		**[$N_{111(2OH)}$][DHP]**	
100 w_1	100 w_2	100 w_1	100 w_2	100 w_1	100 w_2
58.34	4.81	44.35	15.25	36.98	28.75
52.85	7.32	40.92	18.20	32.45	31.22
48.33	9.48	30.32	24.76	31.31	31.41
43.71	10.75	15.29	35.18	22.39	37.44
38.18	14.68			20.94	38.10
34.17	17.43				
30.16	20.38				
27.19	22.55				
23.76	25.39				
21.94	26.82				
19.45	28.90				
17.36	30.62				
14.41	33.08				
11.81	35.44				
10.49	36.40				
9.36	37.58				

Table S2. Experimental binodal data for the system composed of PEG 600 (1) + K_3PO_4 (2) + H_2O (3) at 25 °C and atmospheric pressure.

PEG 600 + K_3PO_4 + H_2O							
100 w_1	100 w_2	100 w_1	100 w_2	100 w_1	100 w_2	100 w_1	100 w_2
58.82	0.87	31.30	5.57	20.97	9.12	14.59	12.34
53.01	1.77	29.78	5.93	19.87	9.54	13.42	12.97
39.34	3.65	26.88	6.78	18.90	9.99	12.58	13.38
36.70	4.22	25.15	7.50	17.78	10.60	11.91	13.67
34.43	4.64	23.81	8.04	16.63	11.15	11.34	13.97
32.53	5.04	22.26	8.61	15.75	11.49		

Aqueous multiphase systems phase diagrams

Table S3. Electrical conductivity (κ) data for the top-, middle- and bottom-rich phases of the quaternary systems composed of [$N_{111(2OH)}$]-based IL + PEG 600 + K_3PO_4 + H_2O (1:1000 (v:v) dilution).

IL	**Weight fraction composition / (wt %)**			**10^{-3} κ / (μS·cm^{-1})**		
	[*IL*]$_M$	**[*PEG*]$_M$**	**[K_3PO_4]$_M$**	**Top phase**	**Middle phase**	**Bottom phase**
[$N_{111(2OH)}$][Lac]	22.81	21.04	26.03	372.3	135.7	1846.6
[$N_{111(2OH)}$][Gly]	22.94	22.98	22.71	59.2	524.7	1453.8
[$N_{111(2OH)}$][Ace]	23.34	22.85	23.34	364.2	89.1	1793.3
[$N_{111(2OH)}$]Cl	23.96	22.69	23.30	515.3	177.0	1686.7
[$N_{111(2OH)}$][DHP]	19.61	20.77	30.38	4.4	546.1	1302.3

SUPPORTING INFORMATION

Table S4. Experimental phase boundary data for systems composed of [[$N_{111(2OH)}$]Cl + PEG 600] (1) + K_3PO_4 + H_2O at 25 °C and atmospheric pressure.

[[$N_{111(2OH)}$]Cl + PEG 600] + K_3PO_4 + H_2O ($mol_{[N111(2OH)]Cl}/mol_{[N111(2OH)]Cl+PEG}$)							
0.08				**0.31**			
100 w_1	100 w_2	100 w_1	100 w_2	100 w_1	100 w_2	100 w_1	100 w_2
78.98	0.88	13.79	13.22	77.15	1.29	17.96	11.15
61.78	2.21	13.36	13.22	64.04	2.22	17.65	11.30
52.41	2.87	13.04	13.42	54.97	3.14	17.36	11.47
46.60	3.23	12.74	13.67	48.25	3.68	17.06	11.63
38.77	4.39	12.30	13.71	43.21	4.22	16.67	11.66
34.75	5.18	12.04	13.82	39.59	4.84	16.44	11.77
31.93	5.82	11.79	13.98	37.71	5.19	16.21	11.85
30.88	6.10	11.53	14.22	35.74	5.63	15.98	11.96
29.90	6.37	11.17	14.23	34.15	6.06	15.76	12.07
26.82	7.56	10.95	14.41	29.98	6.96	15.54	12.16
25.58	7.93	10.61	14.44	29.19	7.32	15.34	12.28
24.30	8.32	10.43	14.59	27.99	7.62	15.12	12.37
23.46	8.69	10.23	14.74	26.87	7.87	14.93	12.49
22.66	9.01	9.94	14.76	26.37	8.01	14.68	12.53
21.54	9.43	9.76	14.93	25.72	8.37	14.44	12.59
21.10	9.55	9.54	14.90	24.76	8.55	14.26	12.66
20.77	9.82	9.38	15.02	24.20	8.90	14.12	12.78
20.27	9.91	9.23	15.12	23.39	9.13	13.94	12.88
19.95	10.13	9.09	15.25	22.88	9.42	13.67	12.89
19.62	10.33	8.89	15.26	22.13	9.59	13.49	12.99
19.15	10.47	8.73	15.41	21.65	9.84	13.34	13.09
18.86	10.62	8.54	15.43	21.00	9.94	13.17	13.21
18.08	10.97	8.42	15.55	20.59	10.20	12.94	13.18
16.97	11.76	8.30	15.67	19.95	10.33	12.80	13.26
16.39	12.15	8.10	15.68	19.56	10.49	12.69	13.33
15.89	12.44	7.99	15.75	19.17	10.72	12.54	13.40
15.30	12.57	7.88	15.86	18.64	10.79	12.41	13.46
14.65	12.94	7.73	15.83	18.30	11.02	12.29	13.51
14.10	13.03						

SUPPORTING INFORMATION

Table S5. Experimental phase boundary for systems composed of [[$N_{111(2OH)}$]Cl + PEG 600] (1) + K_3PO_4 + H_2O at 25 °C and atmospheric pressure.

[[$N_{111(2OH)}$]Cl + PEG 600] + K_3PO_4 + H_2O ($mol_{[N111(2OH)]Cl}/mol_{[N111(2OH)]Cl+PEG}$)							
0.49				**0.55**			
100 w_1	100 w_2	100 w_1	100 w_2	100 w_1	100 w_2	100 w_1	100 w_2
44.52	4.65	8.19	15.62	58.23	3.13	16.85	12.36
36.59	5.79	8.02	15.66	54.23	3.83	16.64	12.47
31.29	7.19	7.72	15.74	49.31	4.32	16.18	12.65
28.91	8.15	7.64	15.75	44.61	4.81	15.88	12.65
26.80	8.75	7.53	15.73	42.11	5.36	15.74	12.72
25.05	9.38	7.45	15.92	40.01	5.68	15.57	12.82
23.49	9.88	7.29	16.01	37.74	6.23	15.41	12.89
22.03	10.30	7.16	16.04	35.66	6.56	15.25	13.01
20.82	10.61	7.05	16.14	34.11	6.90	15.00	13.03
19.84	10.91	6.93	16.12	31.35	7.64	14.86	13.14
19.01	11.45	6.83	16.18	30.04	8.04	14.65	13.15
16.30	12.00	6.73	16.27	28.92	8.33	14.11	13.43
16.04	12.18	6.60	16.30	27.91	8.52	13.96	13.54
15.36	12.51	6.49	16.36	27.10	8.88	13.73	13.48
14.19	12.99	6.41	16.39	26.48	9.23	13.58	13.55
13.80	13.22	6.35	16.53	25.54	9.50	13.39	13.53
13.32	13.49	6.22	16.48	24.23	9.96	13.29	13.61
12.87	13.68	6.14	16.53	23.59	10.07	13.17	13.69
12.50	13.68	6.03	16.55	22.78	10.25	13.05	13.75
12.17	13.91	5.95	16.63	22.30	10.50	12.86	13.73
11.81	14.06	5.88	16.71	21.71	10.57	12.60	13.99
10.89	14.28	5.79	16.74	21.33	10.80	12.47	14.07
10.20	14.48	5.71	16.83	20.71	10.94		
10.02	14.61	5.63	16.85	20.38	11.05		
9.83	14.76	5.54	16.83	20.03	11.23		
9.62	14.78	5.49	16.96	19.67	11.42		
9.43	14.95	5.41	16.98	19.26	11.47		
9.24	14.97	5.34	16.94	19.00	11.64		
9.07	15.12	5.28	17.00	18.54	11.70		
8.90	15.23	5.23	17.06	18.27	11.82		
8.74	15.33	5.16	17.16	18.03	11.91		
8.57	15.45	5.07	17.09	17.83	12.08		
8.41	15.39	5.02	17.13	17.42	12.20		
8.29	15.43	4.98	17.23	17.06	12.23		

SUPPORTING INFORMATION

Table S6. Experimental phase boundary for systems composed of [[$N_{111(2OH)}$]Cl + PEG 600] (1) + K_3PO_4 + H_2O at 25 °C and atmospheric pressure.

[[$N_{111(2OH)}$]Cl + PEG 600] + K_3PO_4 + H_2O ($mol_{[N111(2OH)]Cl}/mol_{[N111(2OH)]Cl+PEG}$)							
0.82				**0.95**			
100 w_1	100 w_2	100 w_1	100 w_2	100 w_1	100 w_2	100 w_1	100 w_2
63.99	4.52	19.85	14.25	72.72	3.76	17.03	19.41
59.65	5.30	19.51	14.38	61.63	4.78	16.64	19.32
55.77	5.80	19.16	14.49	53.66	5.43	16.38	19.39
53.47	6.35	18.88	14.68	50.19	6.42	16.03	19.37
50.69	6.70	18.57	14.82	47.24	7.15	15.43	19.44
47.83	7.01	18.09	14.89	44.91	8.25	15.11	19.46
46.30	7.52	17.81	15.01	43.11	9.17	14.84	19.52
44.65	8.00	17.54	15.10	39.28	10.10	14.51	19.45
43.02	8.35	17.27	15.20	38.41	10.70	14.27	19.56
41.66	8.81	16.86	15.18	35.73	11.82	13.99	19.53
39.94	9.00	16.62	15.27	34.77	12.31	13.79	19.66
39.02	9.28	16.38	15.37	33.16	13.35	13.33	19.70
37.89	9.70	16.09	15.61	31.77	14.12	12.94	19.66
34.37	10.51	15.73	15.64	31.05	14.44	12.42	19.76
33.56	10.76	15.51	15.81	29.61	15.52	12.00	19.87
32.80	11.02	15.18	15.83	28.38	16.06	11.69	19.84
32.00	11.22	14.83	15.85	27.70	16.86	11.42	19.93
31.25	11.44	14.65	15.93	26.70	17.45	11.21	19.88
30.15	11.52	14.46	15.96	26.03	17.69	11.06	19.99
29.48	11.75	14.28	16.00	25.09	18.21	10.81	19.97
28.87	11.90	14.05	15.96	23.71	18.43	10.37	20.16
28.32	12.13			23.25	18.52	10.20	20.21
27.54	12.16			22.79	18.65	9.56	20.39
27.08	12.32			21.73	18.80	9.42	20.37
26.49	12.52			21.29	18.84	9.18	20.44
25.67	12.61			21.18	18.95	8.75	20.63
23.19	13.54			20.84	18.98	8.48	20.62
22.75	13.61			19.73	19.24	8.30	20.82
22.43	13.80			19.20	19.28	7.62	21.04
21.96	13.94			18.82	19.40	7.45	20.91
21.28	14.02			18.31	19.35	7.27	21.02
20.87	14.11			17.81	19.32	7.08	21.19
20.44	14.31			17.49	19.42	6.78	21.27

Table S7. Experimental data of the limit between the solid-liquid region and the three phases region for systems composed of $[N_{111(2OH)}]Cl$ (1) + PEG 600 (2) + K_3PO_4 (3) + H_2O (4) at 25 °C and atmospheric pressure.

$x([N_{111(2OH)}]Cl)$	100 w_1	100 w_2	100 w_3	100 w_4
0.25	3.58	46.15	29.89	20.39
	2.67	34.24	36.88	26.21
0.55	12.88	45.64	19.62	21.86
	10.19	35.37	27.50	26.95
	7.71	27.30	35.04	29.96
0.75	26.71	39.51	9.69	24.09
	22.15	31.98	17.86	28.00
	17.44	25.06	25.31	32.19
	13.52	19.38	32.79	34.31
0.85	38.10	28.87	4.52	28.51
	35.74	27.10	9.06	28.10
	28.98	21.78	16.85	32.39
	23.34	17.72	24.70	34.25
	18.05	13.69	31.78	36.49
0.95	50.70	11.48	4.29	33.53
	45.77	10.38	8.10	35.74
	38.06	8.67	15.44	37.84
	29.86	6.78	22.04	41.33
	24.01	5.60	29.41	40.97

Table S8. Experimental data of the limit between the three phases region and the biphasic region for systems composed of $[N_{111(2OH)}]Cl$ (1) + PEG 600 (2) + K_3PO_4 (3) + H_2O (4) at 25 °C and atmospheric pressure.

$x([N_{111(2OH)}]Cl)$	100 w_1	100 w_2	100 w_3	100 w_4
0.25	5.28	63.82	4.64	26.26
	4.55	57.05	8.88	29.52
0.55	13.56	47.95	4.20	34.28
	12.70	44.49	8.47	34.34
	10.40	36.85	15.84	36.92
	8.39	29.13	22.64	39.84
	6.16	21.80	27.98	44.06
0.75	27.29	39.08	4.53	29.10
	23.88	35.32	8.66	32.14
	20.11	29.02	16.21	34.66
	15.89	22.82	23.05	38.24
	12.17	17.44	29.50	40.90
0.85	37.53	28.43	4.45	29.59
	33.99	25.78	8.62	31.61
	28.29	21.26	16.44	34.01
	22.38	16.99	23.68	36.95
	17.08	12.95	30.07	39.90

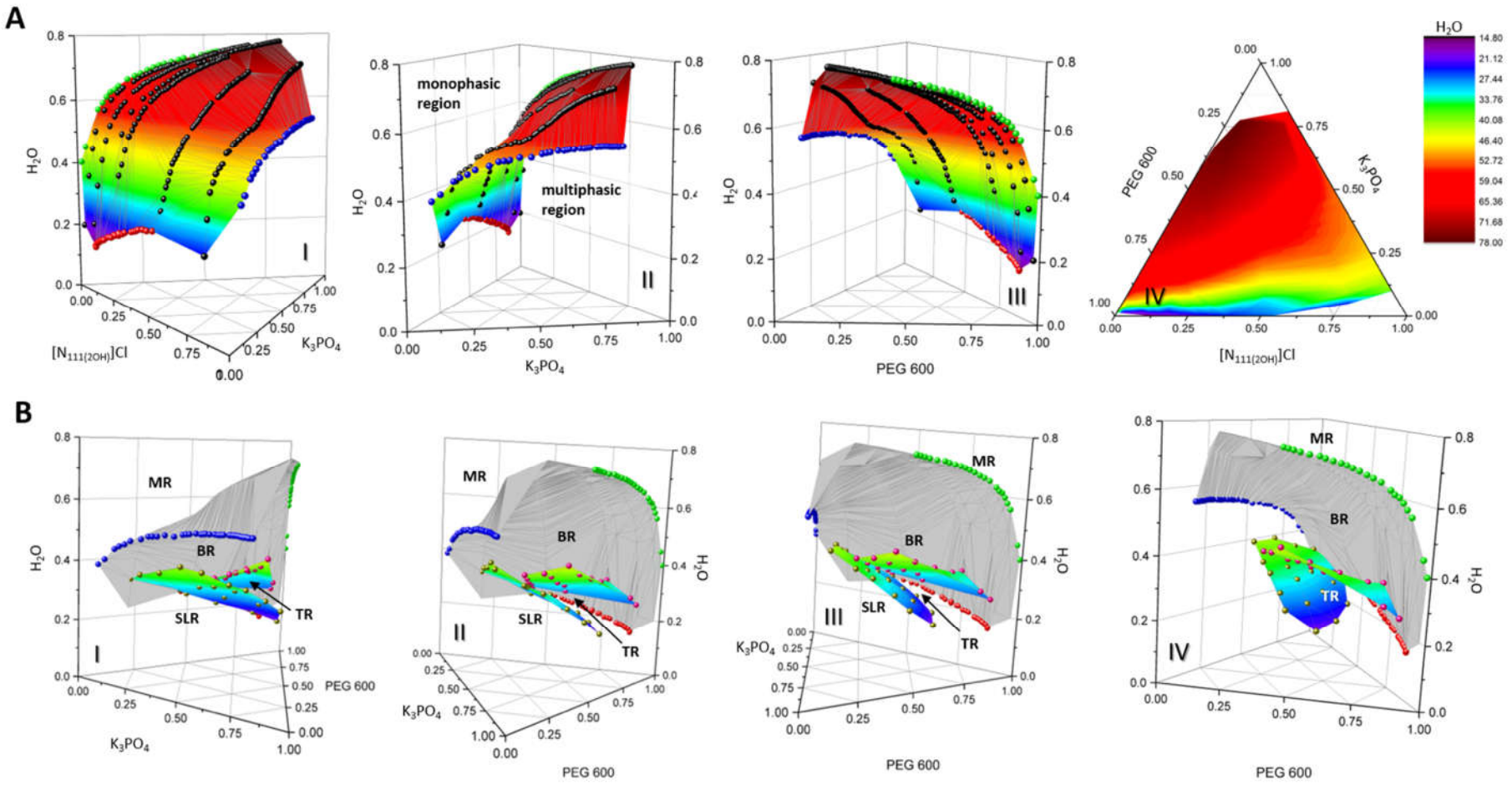

Figure S3. Phase diagram of the MuPS composed of $[N_{111(2OH)}]Cl$ +PEG 600 + K_3PO_4 + H_2O. **(A)** The phase boundary between the monophasic and multiphasic regions from different perspectives – ternary phase diagrams composed of $[N_{111(2OH)}]Cl$ + K_3PO_4 + H_2O (blue dots), PEG 600 + K_3PO_4 + H_2O (green dots), and $[N_{111(2OH)}]Cl$ + PEG 600 + H_2O (red dots), and quaternary mixtures composed of $[N_{111(2OH)}]Cl$ +PEG 600 + K_3PO_4 + H_2O (black dots). **(B)** The limits between the biphasic and triphasic regions (pink dots) and the triphasic and solid-liquid regions (yellow dots) inside the phase boundary (grey surface), from different perspectives. Legend: MR – monophasic region, BR – biphasic region, TR – triphasic region, SLR – solid-liquid region.

Tabel S9. Composition of the coexisting phases of the MuPS composed of 30.70 wt % of [$N_{111(2OH)}$]Cl + 29.64 wt % of PEG 600 + 9.86 wt % of K_3PO_4 + 29.81 wt % of H_2O ("tie surface" 1) and 22.61 wt % of [$N_{111(2OH)}$]Cl + 21.36 wt % of PEG 600 + 22.63 wt % of K_3PO_4 + 33.40 wt % of H_2O ("tie surface" 2).

	MuPS rich phases		
	[$N_{111(2OH)}$]Cl	**PEG 600**	**K_3PO_4**
"tie surface" 1			
[$N_{111(2OH)}$]Cl (wt %)	41.72 ± 2.00	29.89 ± 0.48	0.56 ± 0.02
PEG 600 (wt %)	25.52 ± 1.40	43.36 ± 3.63	7.92 ± 0.32
K_3PO_4 (wt %)	4.36 ± 0.35	4.67 ± 0.31	53.00 ± 4.9
H_2O (wt %)	28.40 ± 0.07	22.08 ± 0.32	39.08 ± 0.18
"tie surface" 2			
[$N_{111(2OH)}$]Cl (wt %)	45.31 ± 1.34	20.46 ± 0.83	1.21 ± 0.01
PEG 600 (wt %)	22.28 ± 0.53	56.82 ± 3.21	14.02 ± 0.02
K_3PO_4 (wt %)	3.00 ± 0.08	4.60 ± 0.51	55.72 ± 5.43
H_2O (wt %)	29.41 ± 0.14	18.10 ± 0.10	30.29 ± 0.04

Table S10. Composition of the ions in the coexisting phases of the MuPS composed of 30.70 wt % of [$N_{111(2OH)}$]Cl + 29.64 wt % of PEG 600 + 9.86 wt % of K_3PO_4 + 29.81 wt % of H_2O ("tie surface" 1).

		MuPS rich phases		
Component	**Ion**	**[$N_{111(2OH)}$]Cl**	**PEG 600**	**K_3PO_4**
[$N_{111(2OH)}$]Cl	**[$N_{111(2OH)}$]$^+$ (mol)**	$(8.52 \pm 0.25) \times 10^{-2}$	$(1.45 \pm 0.02) \times 10^{-2}$	$(1.45 \pm 0.06) \times 10^{-4}$
	Cl^- (mol)	$(5.15 \pm 0.24) \times 10^{-2}$	$(1.20 \pm 0.02) \times 10^{-2}$	$(5.60 \pm 0.26) \times 10^{-4}$
K_3PO_4	**K^+ (mol)**	$(6.16 \pm 0.49) \times 10^{-5}$	$(6.60 \pm 0.43) \times 10^{-5}$	$(2.70 \pm 0.18) \times 10^{-2}$
	$3PO_4^-$ (mol)	$(4.26 \pm 0.12) \times 10^{-5}$	$(1.06 \pm 0.13) \times 10^{-5}$	$(3.42 \pm 0.33) \times 10^{-2}$

Table S11. Composition of ions in the coexisting phases of the MuPS composed of and 22.61 wt % of [$N_{111(2OH)}$]Cl + 21.36 wt % of PEG 600 + 22.63 wt % of K_3PO_4 + 33.40 wt % of H_2O ("tie surface" 2).

		MuPS rich phases		
Component	**Ion**	**[$N_{111(2OH)}$]Cl**	**PEG 600**	**K_3PO_4**
[$N_{111(2OH)}$]Cl	**[$N_{111(2OH)}$]$^+$ (mol)**	$(5.95 \pm 0.12) \times 10^{-2}$	$(8.31 \pm 0.34) \times 10^{-3}$	$(9.57 \pm 0.06) \times 10^{-4}$
	Cl^- (mol)	$(5.88 \pm 0.04) \times 10^{-2}$	$(1.47 \pm 0.00) \times 10^{-2}$	$(4.61 \pm 0.13) \times 10^{-3}$
K_3PO_4	**K^+ (mol)**	$(4.23 \pm 0.12) \times 10^{-5}$	$(6.53 \pm 0.73) \times 10^{-5}$	$(8.72 \pm 0.53) \times 10^{-2}$
	$3PO_4^-$ (mol)	$(2.63 \pm 0.12) \times 10^{-5}$	$(1.07 \pm 0.10) \times 10^{-5}$	$(9.21 \pm 0.36) \times 10^{-2}$

Table S12. Experimental data of the limit between the three phases region and the biphasic region for systems composed of [$N_{111(2OH)}$]Cl (1) + PEG 600 (2) + K_3PO_4 (3) + H_2O (4) at 45 °C and atmospheric pressure.

***x*([$N_{111(2OH)}$]Cl)**	**100 w_1**	**100 w_2**	**100 w_3**	**100 w_4**
0.55	12.15	42.57	8.11	37.17
	9.83	34.83	14.97	40.37
	8.08	28.05	21.81	42.07
	6.09	21.57	27.69	44.64
0.75	24.95	35.73	4.14	35.19
	18.20	26.27	14.67	40.86
	14.05	20.19	20.39	45.38
	10.70	15.34	25.95	48.01
0.85	31.47	23.87	7.98	36.68
	26.03	19.56	15.13	39.28
	20.54	15.59	21.73	42.13
	15.53	11.78	27.35	45.33

Table S13. Experimental data of the limit between the three phases region and the biphasic region for systems composed of $[N_{111(2OH)}]Cl$ (1) + PEG 600 (2) + K_3PO_4 (3) + H_2O (4) at 65 °C and atmospheric pressure.

$x([N_{111(2OH)}]Cl)$	100 w_1	100 w_2	100 w_3	100 w_4
0.55	8.04	27.92	21.70	42.34
	6.08	21.52	27.63	44.76
0.75	16.93	24.44	13.65	44.97
	13.31	19.12	19.32	48.25
	10.22	14.65	24.79	50.33
0.85	28.18	21.37	7.15	43.31
	23.05	17.33	13.40	46.22
	18.19	13.81	19.25	48.75
	13.80	10.47	24.30	51.42

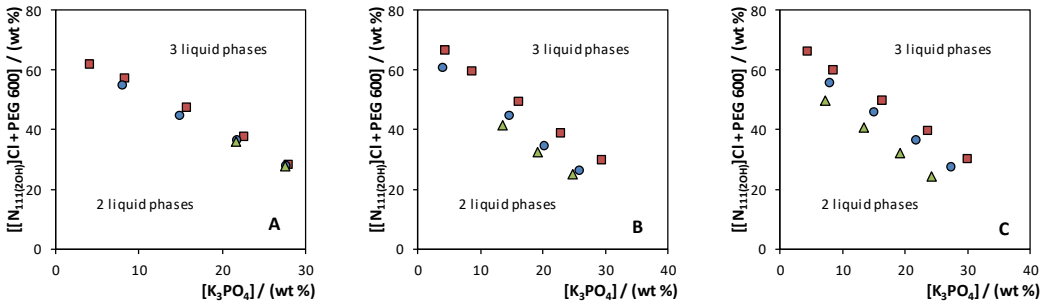

Figure S4. Temperature effect in the three phase region of the MuPS composed of $[N_{111(2OH)}]Cl$ + PEG 600 + K_3PO_4 + H_2O - phase diagram cut at (A) 0.55, (B) 0.75, and (C) 0.85 mol of $[N_{111(2OH)}]Cl$ *per* mol of $[N_{111(2OH)}]Cl$ + PEG 600: 25 °C (■), 45 °C (●), and 65 °C (▲).

Aqueous multiphase systems as separation processes. The reported systems were use in the extraction and selective separation of three textile dyes, namely chloranilic acid, sudan III and PB 27 (presented in the manuscript), as well as for the extraction of tartrazine food dye (E102) and the following biomolecules: -tryptophan, -phenylalanine, -tyrosine, glycine, gallic acid, vanillin, ascorbic acid and caffeine. The results obtained are presented in Figured S5 and S6 and in Table S14.

The extraction of the tartrazine food dye was evaluated in all the MuPS studied in this work. Similarly to the chloranilic acid, tartrazine partitions between the IL- and polymer-rich phases. Nevertheless, its partition is preferential to the IL-rich phase due to its higher hydrophilic character ($\log(K_{OW}) < 0$), with an extraction efficiency higher than 90 % in $[N_{111(2OH)}][Ace]$-based MuPS. Furthermore, it was observed that its extraction to the IL-rich phase is highly depend on the IL chemical nature, decreasing with the IL hydrophilic character, as shown in Figure S5.

As presented in the Table S14, corresponding to the extraction efficiencies of the studied MuPS for other biomolecules, it seems that their performance is ruled by the hydrophilicity/hydrophobicity character of each biomolecule. For example, aromatic amino acids (-tryptophan, -phenylalanine and -tyrosine) are mainly extracted to the IL- and polymer-rich phases. Due to their moderate hydrophilic character, their extraction to the IL-rich phase is higher than 50 %, and presents a linear dependency with their octanol-water partition coefficients values – *cf.* Figure S6. However, it was expected to obtain the preferential extraction of glycine – a linear amino acid, with a high hydrophilic character – to the most hydrophilic phase, the salt-rich phase. Instead, the extraction of this amino acid is very similar to that observed with -tryptophan. This result suggests that the glycine extraction may be ruled by specific interactions occurring between the amino acid and the cholinium-based ILs. This behaviour is in good agreement with the literature[8], where the partition of glycine in zwitterion-salt-based ABS was investigated. When a small alkyl chain zwitterion is used in the ABS formation together with K_3PO_4, glycine presents a preferential partition to the zwitterion-rich phase, suggesting that, despite the high hydrophilicity of this amino acid, its extraction seems to be influenced by specific interactions.

Among the phenolic compounds studied, vanillin is mainly extracted to the polymer-rich phase, while gallic acid presents a favourable partition to the IL-rich phase. Nevertheless, ascorbic acid, partitions among the three-phases of the system, presenting extraction efficiencies of 50.9 % to the $[N_{111(2OH)}]Cl$-rich phase, 25.2 % to the polymer-rich phase, and 23.9 % to the salt-rich phase.

Despite its hydrophilic character, caffeine presents a large extraction efficiency (circa 80 %) to the polymer-rich phase, the most hydrophobic phase of the studied MuPS. This result also suggests that although a strong dependency between the extraction efficiency and the hydrophilicity/hydrophobicity of the biomolecules is present, specific interactions between these molecules and the phase forming components of these systems also play a role on their partition trend.

Overall, these results support the versatility of IL-based MuPS, demonstrating that it is possible to use these systems to selectively separate (bio)molecules of the same family (dyes, amino acids, phenolic compounds, among others) with similar structures and chemical properties, as well as molecules with distinct characteristics.

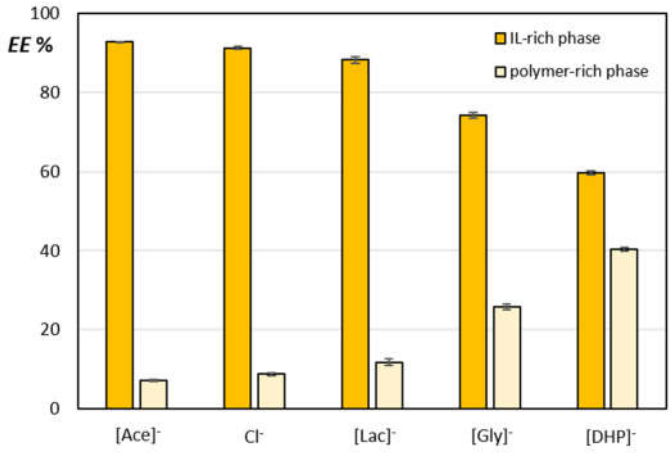

Figure S5. IL anion effect on the selective extraction of tartrazine (E102) dye between the IL- and polymer-rich phases.

Table S14. Extraction of different biomolecules in MuPS composed of $[N_{111(2OH)}]$-based ILs + PEG 600 + K_3PO_4 + H_2O at 25 °C and atmospheric pressure.

Molecule	log(K_{OW})[9]	$[N_{111(2OH)}]$-based MuPS	Extraction efficiency (*EE*) % (± 0.2)		
			$[N_{111(2OH)}]$-rich phase	PEG-rich phase	K_3PO_4-rich phase
-Tryptophan	-1.57	$[N_{111(2OH)}]Cl$	51.1	48.9	0.0
-Phenylalanine	-1.67	$[N_{111(2OH)}]Cl$	64.6	35.4	0.0
-Tyrosine	-1.96	$[N_{111(2OH)}]Cl$	92.2	7.4	0.4
Glycine	-3.89	$[N_{111(2OH)}]Cl$	84.2	15.8	0.0
		$[N_{111(2OH)}][Ace]$	90.4	9.6	0.0
Gallic acid	0.71	$[N_{111(2OH)}]Cl$	85.4	2.0	12.7
Vanillin	1.18	$[N_{111(2OH)}]Cl$	37.0	62.9	0.1
Ascorbic acid	-2.34	$[N_{111(2OH)}]Cl$	50.9	25.2	23.9
		$[N_{111(2OH)}][Ace]$	58.6	13.3	28.1
Caffeine	-0.79	$[N_{111(2OH)}]Cl$	20.5	79.5	0.0

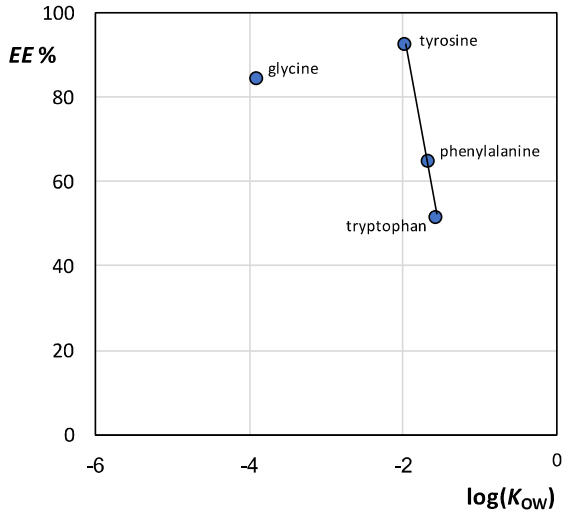

Figure S6. Extraction efficiency (*EE* %) as a function of the log(K_{OW}) of amino acids.

References

[1] N. Muhammad, M. I. Hossain, Z. Man, M. El-Harbawi, M. A. Bustam, Y. A. Noaman, N. B. Mohamed Alitheen, M. K. Ng, G. Hefter, C.-Y. Yin, *J. Chem. Eng. Data* **2012**, *57*, 2191–2196.

[2] J. Pernak, A. Syguda, I. Mirska, A. Pernak, J. Nawrot, A. Pradzyńska, S. T. Griffin, R. D. Rogers, *Chem. - A Eur. J.* **2007**, *13*, 6817–6827.

[3] S. P. M. Ventura, C. M. S. S. Neves, M. G. Freire, I. M. Marrucho, J. Oliveira, J. A. P. Coutinho, *J. Phys. Chem. B* **2009**, *113*, 9304–9310.

[4] C. M. S. S. Neves, S. P. M. Ventura, M. G. Freire, I. M. Marrucho, J. A. P. Coutinho, *J. Phys. Chem. B* **2009**, *113*, 5194–5199.

[5] B. Zavlasky, *Aqueous Two-Phase Partitioning: Physical Chemistry and Bioanalytical Applications*, M. Dekker, New York, **1994**.

[6] D. L. Jones, A. G. Owen, J. F. Farrar, *Soil Biol. Biochem.* **2012**, *34*, 1893–1902.

[7] S. Moore, W. H. Stein, *J. Biol. Chem.* **1954**, *211*, 907–913.

[8] A. M. Ferreira, H. Passos, A. Okafuji, M. G. Freire, J. A. P. Coutinho, H. Ohno, *Green Chem.*, **2017**, *19*, 4012-4016.

[9] ChemSpider – *The free chemical database*, 2015, www.chemspider.com